

PACS 61.46.Hk, 63.22.Kn, 78.30.Am

Laser heating effect on Raman spectra of Si nanocrystals embedded into SiO_x matrix

A.S. Nikolenko

V. Lashkaryov Institute of Semiconductor Physics, NAS of Ukraine, Optical Submicron Spectroscopy Laboratory, 45, prospect Nauky, 03028 Kyiv, Ukraine

E-mail: Nikolenko_mail@ukr.net, phone/fax: +38 (044) 525-64-73

Abstract. Influence of combined size confinement effect and effect of local laser heating on the first-order Raman spectrum of silicon nanocrystals embedded into SiO_x matrix has been studied. Increase of the local temperature of Si nanocrystals caused by laser illumination with the power density up to 10 mW/μm² was estimated from the ratio of the Stokes/anti-Stokes peak intensities. Almost linear dependence of nanocrystals local temperature on the power density of exciting radiation with a rate of 63.6 K·μm²/mW has been found. The phonon line shape at power densities, when no laser heating effect is registered, was shown to be described well within the correlation length model of phonon confinement of Si nanocrystals with the size $L = 9.2$ nm. Observed phonon softening and broadening with increase of the exciting power density is considered as temperature-induced vibration anharmonicity with the decay of optical phonons through three- and four-phonon processes and corresponding anharmonic constants have been determined.

Keywords: silicon nanocrystals, Raman spectroscopy, phonon confinement, laser heating.

Manuscript received 01.11.12; revised version received 05.12.12; accepted for publication 26.01.13; published online 28.02.13.

1. Introduction

The low-dimensional Si nanostructures are considered as promising candidates for large area of photonic and electronic applications such as light-emitters [1, 2], photodetectors with tunable spectral range [3], and solar cells [4]. Due to electron confinement effect, properties of Si nanocrystals (nc - Si) can be modified by changing the crystallite size, shape and surrounding [5, 6]. Reducing the size of Si nanocrystals to values comparable with the Bohr exciton radius leads to band gap widening, conversion to pseudo-direct band gap semiconductor with a high quantum efficiency of emission and strong shift of nc - Si photoluminescence into the visible energy range [7].

Silicon nanocrystals are frequently characterized by means of Raman spectroscopy that provides very detailed information on their crystal structure [8-11]. For bulk Si, triply degenerate (T_{2g}) first-order optical phonon at the Brillouin-zone centre is observed at 521 cm⁻¹. Upon decreasing the crystallite size to nanoscale, the phonon confinement effect significantly modifies

vibrational properties of Si nanocrystals. A phonon confinement model for crystalline silicon thin films was first developed by Richter et al. [12] and later extended by Campbell et al. [13] to account for various material geometries. According to this model, the decrease of Si crystallite sizes less than ~10 nm results in breaking the wavevector Raman scattering selection rule ($\mathbf{q} = 0$) and causes the softening and asymmetric broadening of the T_{2g} phonon Raman peak as compared to that of bulk Si. On the other hand, anharmonicity, due to the local laser heating of the sample, can significantly contribute to the phonon softening and broadening, which leads to overestimation of the quantum confinement effect.

In micro-Raman experiments, a laser power of few milliwatts typically is focused to a spot of several micrometers in diameter, which leads to high power densities of excitation and results in high local temperatures [14]. Laser heating effect can be especially important if taking into account significantly reduced, as compared to bulk Si, heat dissipation in Si nanocrystals embedded into insulating matrix [14, 15]. In this work, the influence of both effects (quantum confinement and

local heating) on the first-order Raman-active phonon peak in Si nanocrystals has been studied using micro-Raman spectroscopy in a wide range of excitation power densities. Such study is important for clearer understanding the thermal stability of Si nanocrystals embedded into oxide matrix under impact of high temperatures and high densities of optical radiation.

2. Experimental

Investigated silicon nanocrystals (nc-Si) in SiO_x matrix were obtained by magnetron co-sputtering from Si and SiO₂ targets on silica substrates. The films were subsequently annealed at 1150 °C in an inert atmosphere. Stokes and anti-Stokes micro-Raman spectra were measured in the backscattering geometry at room temperature in triple subtractive mode of T-64000 Horiba Jobin-Yvon Raman spectrometer, equipped with electrically cooled CCD detector. The line 488 nm of Ar-Kr ion laser with a varied power was used for excitation. Exciting radiation with the power densities of 0.05÷10 mW/μm² was focused on the sample surface with the 100×/0.9 Olympus objective to the spot area about 1 μm². For evaluation of Stokes and anti-Stokes components of Raman spectra, spectral sensitivity of the experimental setup was taken into account. Temperature of the investigated Si nanocrystals was estimated from the intensity ratio of their Stokes and anti-Stokes phonon components.

3. Results and discussion

For better understanding the thermal stability of nc-Si in SiO_x matrix, high-temperature Raman spectroscopy studies were carried out. Fig. 1 shows typical Stokes and anti-Stokes Raman spectra of the investigated Si nanocrystals measured at a varied excitation power density. The main feature of nc-Si Raman spectra is the TO phonon mode, which is always down-shifted and broadened with respect to bulk Si [12]. Increase of the power density from 0.05 up to 10 mW/μm² leads to a gradual low-frequency shift of the nc-Si TO phonon mode from 518.6 down to 494.0 cm⁻¹ and corresponding increase of its full-width (Γ) from 5.4 to 29.3 cm⁻¹. Such drastic modifications of the Raman spectrum with the excitation power can be understood, if to assume significant local heating of Si nanocrystals occurred within the excitation area [14, 16].

Local temperature of Si nanocrystals within the excitation area can be estimated from the ratio of Stokes and anti-Stokes integrated intensities (I_S/I_{AS}) of TO phonon mode according to relation [17, 18]:

$$\frac{I_S}{I_{AS}} = \left(\frac{\omega_l + \omega_S}{\omega_l - \omega_S} \right)^4 \exp\left(\frac{\hbar\omega_S}{kT}\right) \quad (1)$$

where ω_l , ω_S and ω_{AS} are frequencies of exciting photons, Stokes and anti-Stokes phonon components, correspondingly.

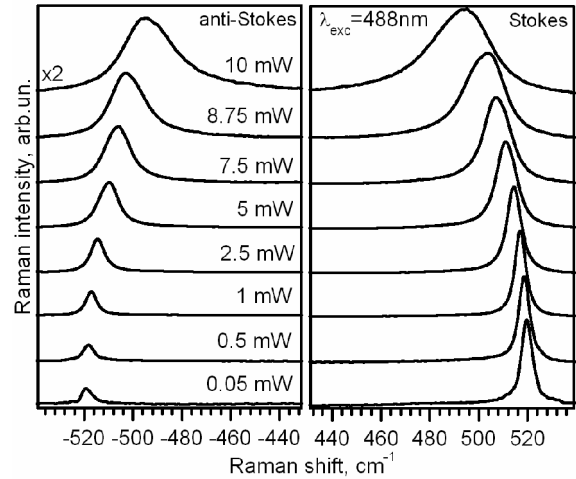


Fig. 1. Normalized Stokes and anti-Stokes Raman spectra measured at varied power densities of exciting radiation ($P_{exc} = 0.05 \div 10 \text{ mW}/\mu\text{m}^2$). $\lambda_{exc} = 488 \text{ nm}$, $T = 300 \text{ K}$. Anti-Stokes Raman spectra are multiplied by factor 2 for convenience reason.

Fig. 2 shows the dependence of nc-Si local temperature on the power density of exciting radiation obtained from the analyses of their Stokes and anti-Stokes Raman spectra according to Eq. (1). As can be seen, increase in the laser exciting power density from 0.05 up to 10 mW/μm² leads to almost linear gradual increase in nc-Si local temperature from about 300 K to almost 920 K. Such a high value of local temperature at a relatively low laser power can be related with low heat dissipation in the system of Si nanocrystals embedded into SiO_x matrix, which is caused both by rather low thermal conductivity of SiO_x matrix (thermal conductivity of SiO₂ makes only 1.4 Wm⁻¹K⁻¹ in contrast to 156 Wm⁻¹K⁻¹ for bulk Si at 300 K [19]) and low thermal conductivity of the whole nc-Si/SiO_x system, which is limited by phonon scattering on grain boundaries, interfaces and structural defects [14, 15]. Also, it should be mentioned that at the lowest excitation power densities ($P < 0.5 \text{ mW}/\mu\text{m}^2$) no laser heating of the investigated Si nanocrystals occurs. So, to exclude temperature effects for further analysis of the nc-Si TO phonon line shape, Raman spectra measured at the lowest power density were used.

The detailed view of Raman spectra measured at the excitation power density 0.05 mW/μm² is shown in Fig. 3. As can be seen, the TO phonon line observed at $\omega = 518.6 \text{ cm}^{-1}$ is down-shifted and broadened ($\Gamma = 5.4 \text{ cm}^{-1}$) as compared to bulk Si, and has significant asymmetry with low-frequency tailing, which is typical for Si nanocrystals. For spherical nanocrystals with the diameter L , phonon damping $\exp(-q^2 L^2 / 16\pi^2)$ and neglecting the size dispersion of nanocrystals, the Raman intensity of the optical phonon line can be

expressed using the correlation length model of strong phonon confinement [12, 13]:

$$I(\omega) = \int_0^{2\pi/a} \frac{\exp(-q^2 L^2 / 16\pi^2)}{[\omega - \omega(q)]^2 + (\Gamma_0 / 2)^2} d^3 q \quad (2)$$

where q is the phonon wavevector in $2\pi/a_0$ units ($a_0 = 0.357$ nm – silicon lattice parameter [20]), $\omega(q)$ – dispersion relation for TO phonons in Si, which can be approximated by the relation $\omega^2(q) = A + B \cos(aq/4)$, with $A = 1.714 \cdot 10^5 \text{ cm}^{-2}$ and $B = 1.000 \cdot 10^5 \text{ cm}^{-2}$ [21], and Γ_0 – natural line width (3.6 cm^{-1} for Si). From simulation of the experimental Raman spectrum (Fig. 3) by using Eq. (2), it was found that the average size of Si nanocrystals makes $L = 9.2$ nm. However, the frequency position of experimental phonon line appeared to be down-shifted to 1.1 cm^{-1} relatively to the simulated Raman line. The additional down-shift of the nc-Si phonon band can be caused by presence of tensile strains, which can arise both on nc-Si/SiO_x and nc-Si film/silica substrate interfaces due to difference in thermal expansion coefficients [22]. In the case of hydrostatic strains, the shift of Si phonon bands with the strain can be expressed as [23, 24]:

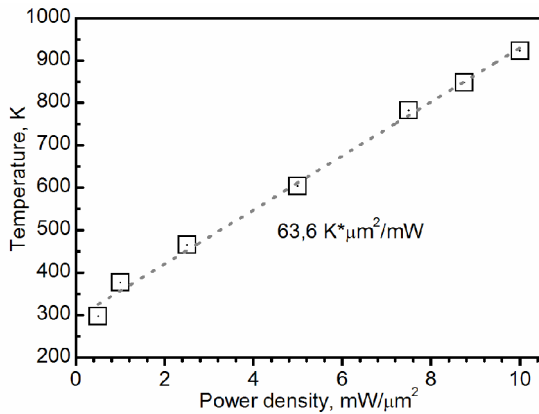


Fig. 2. Dependence of Si nanocrystals local temperature on the power density of exciting radiation. $\lambda_{\text{exc}} = 488$ nm.

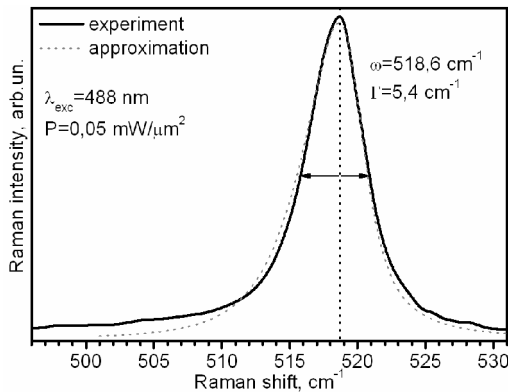


Fig. 3. Raman spectrum of Si nanocrystals measured at the excitation power density $0.05 \text{ mW}/\mu\text{m}^2$. $\lambda_{\text{exc}} = 488$ nm, $T = 300$ K.

$$\Delta\omega(\sigma) = \frac{\sigma}{2\omega_0} [(S_{11} + 2S_{12})(p + 2q)], \quad (3)$$

where ω_0 is the LO-TO phonon frequency of strain-free silicon, $S_{11} = 7.68 \cdot 10^{-12} \text{ Pa}^{-1}$, $S_{12} = -2.14 \cdot 10^{-12} \text{ Pa}^{-1}$, $p = -1.43\omega_0^2$, $q = -1.89\omega_0^2$ [24]. Estimation of deformation using Eq. (3) and obtained value $\Delta\omega = 1.1 \text{ cm}^{-1}$ gives tensile strains in Si nanocrystals of 0.24 GPa .

Fig. 4 shows temperature dependences of the nc-Si optical phonon frequency (ω) and half-width (Γ), where the typically low-frequency shift and phonon mode broadening with temperature are observed [14, 16, 25]. As the vibrational potential includes anharmonic terms, generated optical phonons can decay into low-energy phonons. When the temperature increases, the decay processes intensify, resulting in an increased full-width of the Raman peak. Moreover, increase of the lattice parameter results in weakening the bonds between atoms, which leads to the low-frequency shift of the phonon modes. Below the Debye temperature, decay of optical phonons occurs within the three-phonon process (anharmonicity with a cubic degree) on two acoustical phonons with opposite wave vectors [17, 26]. At temperatures higher than the Debye temperature ($T_D = 645$ K for bulk Si), when all the phonon modes are excited and temperature increase is accompanied with increase of vibrational amplitudes, also quartic anharmonicity should be taken into account and corresponding four-phonon process should be considered. In case of Si nanocrystals temperature dependence of phonon line width and frequency in a wide temperature range can be written as [18]:

$$\Gamma(T) = A \left(1 + \frac{2}{e^x - 1} \right) + B \left(1 + \frac{3}{e^y - 1} + \frac{3}{(e^y - 1)^2} \right) + \Gamma_1 \quad (4)$$

$$\omega(T) = \omega_0 + C \left(1 + \frac{2}{e^x - 1} \right) + D \left(1 + \frac{3}{e^y - 1} + \frac{3}{(e^y - 1)^2} \right) - \Delta\omega_1 \quad (5)$$

where $x = h\omega_0 / 2kT$, $y = h\omega_0 / 3kT$; A , B , C and D – anharmonic constants, Γ_1 is additional line broadening and $\Delta\omega_1$ is the additional frequency shift due to the phonon confinement effect and elastic strains.

In our case, the temperature dependence of the phonon line width and frequency (Fig. 4) can be separated into two temperature regions. The first region ($T < 800$ K) is characterized by slow increase (decrease) of the line width (frequency) with temperature, which are well approximated by the equations (4) and (5) with the values of anharmonic constants $A = 1.15$, $B = 0.25$, $C = -2.62$

and $D = -0.19$, confirming the phonon decay mechanisms in three-phonon (cubic anharmonicity degree) and four-phonon process (cubic and quartic anharmonicity).

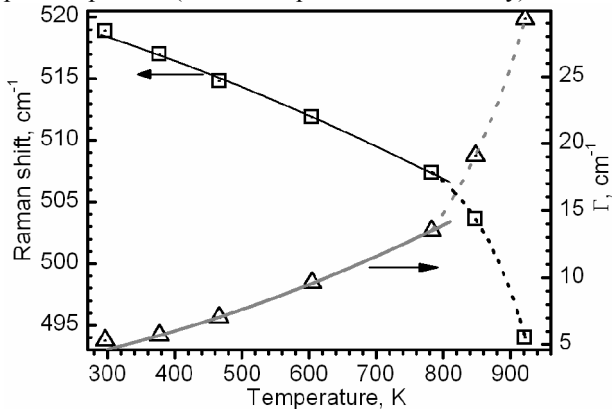


Fig. 4. Temperature dependence of the nc-Si TO phonon mode frequency and full-width. Dashed curves are shown as guide to the eye.

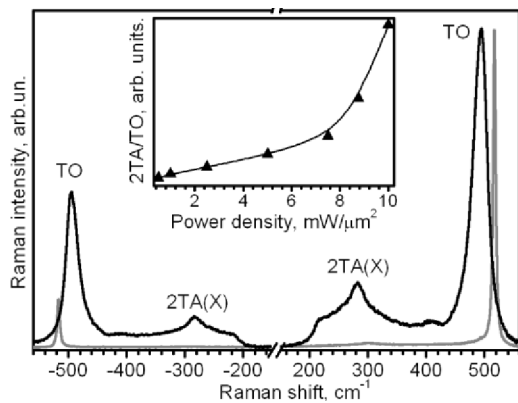


Fig. 5. Stokes and anti-Stokes Raman spectra of Si nanocrystals measured at the excitation power densities 1 and 10 $\text{mW}/\mu\text{m}^2$.

At high temperatures ($T > 800$ K), quite different behavior of temperature dependences with drastic increase (decrease) of phonon line width (frequency) is observed. At temperature increase to 920 K phonon line broadens up to 29 cm^{-1} and shifts down to 494 cm^{-1} . This significant modification of the phonon spectra at relatively low temperatures (for comparison, such temperature-induced line shift and broadening for bulk Si occur at temperatures about 1200 K [18]) is quite unusual and could be explained only if additional mechanisms of phonon decay and heat dissipation in Si nanocrystals are taken into account.

Significant modification of the phonon spectrum at high power of excitation, where intensive 2TA(X) peak is registered in anti-Stokes region (Fig. 5) with increasing the relative intensity (as compared to TO peak) with the excitation power (see inset in Fig. 5) could be an evidence of significant excitation of the phonon system as well as effective decay of optical

phonons into low-frequency acoustical phonons at temperatures higher than the Debye one (the latter for nanocrystals is expected to be lower than that for bulk crystals [27]). In systems excited in such a manner, anharmonicity of phonon vibrations may additionally influence the scattering process. For example, it may lead to breakdown of selection rules and allows phonons with the non-zero wave vector contribute to Raman process resulting in additional phonon line asymmetric broadening and low-frequency shift. Another possible reason of unusual phonon line broadening could be a result of observed at high powers of excitation Fano interaction involving optical phonons and photoexcited electrons [28, 29]. Additional optical phonon decay channels can be also related with the anharmonicity of low-frequency acoustical phonons [11] or surface phonon modes [15]. The additional process of energy dissipation could be also through black body emission of heated Si nanoparticles [14]. More detailed analysis of the influence of mentioned above mechanisms on the phonon spectrum requires further investigations.

4. Conclusions

In this work, micro-Raman spectra of Si nanocrystals produced by the magnetron sputtering technique, measured at varied excitation power densities have been analyzed in details. The dependence of Si nanocrystals local temperature on the power density of exciting radiation is found to be linear with the rate $63.6 \text{ K}\cdot\mu\text{m}^2/\text{mW}$. The phonon line shape at the lowest power density, when no laser heating effect is registered, was shown to be described well within the correlation length model of phonon confinement. Observed large phonon softening and broadening with exciting power density are due to the laser heating effect. The temperature dependence of the Si nanocrystal optical phonon mode in the temperature range $T < 800$ K is shown to be dominated by the anharmonic effects through the three- and four-phonon decay processes, while confinement plays a secondary role. However, for higher temperatures, where drastic phonon softening and broadening are observed, additional phonon decay and energy dissipation mechanisms should be considered.

4. Acknowledgement

Author would like to thanks Dr. Viktor Strelchuk for helpful discussion of the results and acknowledge the financial support from the State Program of Ukraine "Nanotechnologies and Nanomaterials" through the Project #3.5.2.6/48.

References

1. R. Collins, P.M. Fauchet, and M.A. Tischler, Porous silicon: From luminescence to LEDs // *Phys. Today*, **50**, p. 24 (1997).

2. K.D. Hirschman, L. Tsybeskov, S.P. Duttagupta, and P.M. Fauchet, Silicon-based visible light-emitting devices integrated into microelectronic circuits // *Nature*, **384**, p. 338 (1996).
3. Z. Huang, James E. Carey, Mingguo Liu, Xiangyi Guo, Eric Mazur, Joe C. Campbell, Microstructured silicon photodetector // *Appl. Phys. Lett.* **89**, 033506 (2006).
4. S. Park, E. Cho, D. Song, G. Conibeer, M.A. Green, n-type silicon quantum dots and p-type crystalline silicon heteroface solar cells // *Solar Energy Materials and Solar Cells*, **93**(6-7), p. 684 (2009).
5. Md.N. Islam, Satyendra Kumar, Influence of surface states on the photoluminescence from silicon nanostructures // *J. Appl. Phys.* **93**, p. 1753 (2003).
6. X.X. Wang, J.G. Zhang, L. Ding, B.W. Cheng, W.K. Ge, J.Z. Yu, and Q.M. Wang, Origin and evolution of photoluminescence from Si nanocrystals embedded in a SiO₂ matrix // *Phys. Rev. B*, **72**, 195313 (2005).
7. M.V. Wolkin, J. Jorne, P.M. Fauchet, G. Allan and C. Delerue, Electronic states and luminescence in porous silicon quantum dots: The role of oxygen // *Phys. Rev. Lett.* **82**, p. 197 (1999).
8. A.S. Nikolenko, M.V. Sopinsky, V.V. Strelchuk, L.I. Veligura, V.V. Gomonovych, Raman study of Si nanoparticles formation in the annealed SiO_x and SiO_x:Er,F films on sapphire substrate // *J. Optoelectron. and Adv. Mater.* **14**(1-2), p. 120 (2012).
9. S. Hernández, A. Martínez, P. Pellegrino, Y. Lebour, B. Garrido, E. Jordana, and J.M. Fedeli, Silicon nanocluster crystallization in SiO_x films studied by Raman scattering // *J. Appl. Phys.* **104**, 044304 (2008).
10. T. Arguirov, T. Mchedlidze, M. Kittler, R. Rolver, B. Berghoff, M. Forst, B. Spangenberg, Residual stress in Si nanocrystals embedded in a SiO₂ matrix // *Appl. Phys. Lett.* **89**, 053111 (2006).
11. G. Viera, S. Huet, L. Boufendi, Crystal size and temperature measurements in nanostructured silicon using Raman spectroscopy // *J. Appl. Phys.* **90**(8), p. 4175 (2001).
12. H. Richter, Z.P. Wang, and L. Ley, The one phonon Raman spectrum in microcrystalline silicon // *Solid State Communs.* **39**(5), p. 625 (1981).
13. I.H. Campbell, P.M. Fauchet, The effects of microcrystal size and shape on the one phonon Raman spectra of crystalline semiconductors // *Solid State Communs.* **58**(10), p. 739 (1984).
14. V. Poborchii, Tetsuya Tada, and Toshihiko Kanayama, Giant heating of Si nanoparticles by weak laser light: Optical microspectroscopic study and application to particle modification // *J. Appl. Phys.* **97**, 104323 (2005).
15. G. Faraci, Santo Gibilisco, Agata R. Pennisi, Superheating of silicon nanocrystals observed by Raman spectroscopy // *Phys. Lett. A*, **373**, p. 3779 (2009).
16. J. Menendez, and M. Cardona, Temperature dependence of the first-order Raman scattering by phonons in Si, Ge, and a-Sn: Anharmonic effects // *Phys. Rev. B*, **29**(4), p. 2051 (1984).
17. T.R. Hart, R.L.A., and Benjamin Lax, Temperature dependence of Raman scattering in silicon // *Phys. Rev. B*, **1**(2), p. 638 (1970).
18. M. Balkanski, R.F.W., and E. Haro, Anharmonic effects in light scattering due to optical phonons in silicon // *Phys. Rev. B*, **28**(4), p. 1928 (1983).
19. S.M. Sze, *Physics of Semiconductor Devices*. John Wiley and Sons, Inc, New York, 1981.
20. M.E. Straumanis, E.Z. Aka, Lattice parameters, coefficients of thermal expansion, and atomic weights of purest silicon and germanium // *J. Appl. Phys.* **23**, p. 330 (1952).
21. R. Tubino, L. Piseri, G. Zerbi, Lattice dynamics and spectroscopic properties by a valence force potential of diamondlike crystals: C, Si, Ge and Sn // *J. Chem. Phys.* **56**(3), p. 1022 (1972).
22. G. Lucovsky, J.C. Phillips, Interfacial strain-induced self-organization in semiconductor dielectric gate stacks. I. Strain relief at the Si-SiO₂ interface // *J. Vac. Sci. Technol. B*, **22**(4), p 2087 (2004).
23. I. De Wolf, Micro-Raman spectroscopy to study local mechanical stress in silicon integrated circuits // *Semicond. Sci. Technol.* **11**, p. 139-154 (1996).
24. E. Anastassakis, A. Pinczuk, E. Burstein, F.H. Pollak and M. Cardona, Effect of static uniaxial stress on the Raman spectrum of silicon // *Solid State Communs.* **8**(2), p. 133 (1970).
25. R. Kumar, A.K. Shukla, Temperature dependent phonon confinement in silicon nanostructures // *Phys. Lett. A*, **373**, p. 133 (2008).
26. P. Mishra, and K.P. Jain, Temperature-dependent Raman scattering studies in nanocrystalline silicon and finite-size effects // *Phys. Rev. B*, **62**(22), p. 14790 (2000).
27. X.X. Yang, Z.F. Zhou, Y. Wang, R. Jiang, W.T. Zheng, and Chang Q. Sun, Raman spectroscopy determination of the Debye temperature and atomic cohesive energy of CdS, CdSe, Bi₂Se₃, and Sb₂Te₃ nanostructures // *J. Appl. Phys.* **112**, 083508 (2012).
28. A.K. Shukla, Rajesh Kumar, and Vivek Kumar, Electronic Raman scattering in the laser-etched silicon nanostructures // *J. Appl. Phys.* **107**, 014306 (2010).
29. R. Gupta, Q. Xiong, C.K. Adu, U.J. Kim, and P.C. Eklund, Laser-induced Fano resonance scattering in silicon nanowires // *Nano Lett.* **3**(5), p. 627 (2003).